



FEN1 is a prognostic biomarker for ER+ breast cancer and associated with tamoxifen resistance through the ER α /cyclin D1/Rb axis

Lu Xu^{1,2}, Ji-Ming Shen^{1,2}, Jing-Lei Qu^{1,2}, Na Song^{1,2}, Xiao-Fang Che^{1,2}, Ke-Zuo Hou^{1,2}, Jing Shi^{1,2}, Lei Zhao^{1,2}, Sha Shi^{1,2}, Yun-Peng Liu^{1,2}, Xiu-Juan Qu^{1,2}, Yue-E Teng^{1,2}

¹Department of Medical Oncology, the First Hospital of China Medical University, Shenyang, China; ²Key Laboratory of Anticancer Drugs and Biotherapy of Liaoning Province, the First Hospital of China Medical University, Shenyang, China

Contributions: (I) Conception and design: L Xu, JM Shen, JL Qu; (II) Administrative support: XJ Qu, YE Teng; (III) Provision of study materials or patients: L Xu, JM Shen; (IV) Collection and assembly of data: L Xu, JM Shen; (V) Data analysis and interpretation: L Xu; (VI) Manuscript writing: All authors; (VII) Final approval of manuscript: All authors.

Correspondence to: Yue-E Teng; Xiu-juan Qu. Department of Medical Oncology, the First Hospital of China Medical University, No. 155 Nanjingbei Road, Shenyang 110001, China. Email: yeteng@cmu.edu.cn; xiujuanqu@yahoo.com.

Background: Tamoxifen is an important choice in endocrine therapy for patients with oestrogen receptor-positive (ER+) breast cancer, and disease progression-associated resistance to tamoxifen therapy is still challenging. Flap endonuclease-1 (FEN1) is used as a prognostic biomarker and is considered to participate in proliferation, migration, and drug resistance in multiple cancers, especially breast cancer, but the prognostic function of FEN1 in ER+ breast cancer, and whether FEN1 is related to tamoxifen resistance or not, remain to be explored.

Methods: On-line database Kaplan-Meier (KM) plotter, GEO datasets, and immunohistochemistry were used to analyse the prognostic value of FEN1 in ER+ breast cancer from mRNA and protein levels. Cell viability assay and colony formation assays showed the response of tamoxifen in MCF-7 and T47D cells. Microarray data with FEN1 siRNA *versus* control group in MCF-7 cells were analysed by Gene Set Enrichment Analysis (GSEA). The protein levels downstream of FEN1 were detected by western blot assay.

Results: ER+ breast cancer patients who received tamoxifen for adjuvant endocrine therapy with poor prognosis showed a high expression of FEN1. MCF-7 and T47D appeared resistant to tamoxifen after FEN1 over-expression and increased sensitivity to tamoxifen after FEN1 knockdown. Importantly, FEN1 over-expression could activate tamoxifen resistance through the ER α /cyclin D1/Rb axis.

Conclusions: As a biomarker of tamoxifen effectiveness, FEN1 participates in tamoxifen resistance through ER α /cyclin D1/Rb axis. In the future, reversing tamoxifen resistance by knocking-down FEN1 or by way of action as a small molecular inhibitor of FEN1 warrants further investigation.

Keywords: Estrogen receptor positive (ER+) breast cancer; Flap endonuclease-1 (FEN1); prognostic biomarker; tamoxifen resistance

Submitted Apr 02, 2020. Accepted for publication Oct 12, 2020.

doi: 10.21037/atm-20-3068

View this article at: <http://dx.doi.org/10.21037/atm-20-3068>

Introduction

Breast cancer is the most common malignant tumour occurring in women (1,2). Roughly 70–75% of breast cancers are oestrogen receptor-positive (ER+) and effective

anti-ER endocrine therapy has brought benefits to reduce cancer-related mortality. Tamoxifen, an ER antagonist, remains an important choice for endocrine therapy in patients with ER+ breast cancer (3-5). Unfortunately,

approximately 30% of women eventually relapses and dies due to the emergence of tamoxifen resistance (6,7). Previous studies have shown that the ER α pathway interacts with DNA damage responses and DNA repair reactive kinases, increasing genomic instability and causing failure of breast cancer treatment (8,9). Therefore, in-depth exploration of DNA damage repair systems and related mechanisms of tamoxifen resistance has important clinical value for overcoming tamoxifen resistance in patients with ER+ breast cancer.

Flap endonuclease-1 (FEN1) is a highly conserved structure-specific nuclease and possesses multiple activities including flap endonuclease, 5'-exonuclease and gap-endonuclease, which allow FEN1 to play an essential role in Okazaki fragment maturation, long-patch base excision repair, stalled replication fork rescue, telomere maintenance, and apoptotic DNA fragmentation (10-16): because the lack of the activity of FEN1 nuclease leads to the initiation of cancer, FEN1 is generally regarded as a tumour suppressor in maintaining the integrity of genomes (17,18). However, partially due to its essential role in DNA replication and repair, over-expression of FEN1 confers proliferation, migration, and drug resistance in cancer cells (10,19-26). A higher FEN1 expression level could be observed in multiple types of cancer, including breast cancer, which is related to poor differentiation and poor prognosis (22,27-31). In addition, our group also found that over-expression of FEN1 can promote breast cancer cells in terms of proliferation, migration, and drug resistance (21,24,32). Although functions of FEN1 in activating cancer progression are characterised extensively and FEN1 interactions with ER α have been studied (8,33), few researchers have investigated the function and molecular mechanisms of FEN1-mediated endocrine therapy resistance.

In this study, we present evidence suggesting that FEN1 is a prognostic biomarker for patients with ER+ breast cancer, especially in predicting disease recurrence and overall survival (OS) of these patients with adjuvant tamoxifen therapy through on-line database and IHC analysis from samples collected in our center. Then, we found that FEN1 rendered the ER+ breast cancer cells insensitive to the growth inhibitory effects of tamoxifen *in vitro*, which was associated with the activation of the ER α /cyclin D1/Rb axis. These findings provide better evidence as to how FEN1 contributes to tamoxifen resistance and serves as a critical regulator in activation of the ER α /cyclin D1/Rb axis.

We present the following article in accordance with the REMARK reporting checklist (available at <http://dx.doi.org/10.21037/atm-20-3068>).

Methods

The study was conducted in accordance with the Declaration of Helsinki (as revised in 2013). The study was approved by institutional/regional/national ethics/committee/ethics board of the first hospital of China Medical University (No. [2016]120: the registration number of ethics board) and informed consent was taken from all the patients.

Kaplan-Meier (KM) plotter analysis

We used KM Plotter (<http://kmplot.com/analysis/>), a database that integrates gene expression data and clinical data, to obtain survival data for breast cancer, in relation to expression levels of genes of interest (34). Kaplan Meier plotter has information of 54,675 genes on survival, including 5,143 breast, 1816 ovarian, 2,437 lung and 1,065 gastric cancer patients with a mean follow-up of 69/40/49/33 months, respectively.

Briefly, the best specific probes (JetSet probes) for FEN1 (Affy ID:204767_s_at) was entered to obtain KM plots. Information on relapse free survival (RFS) and overall patient survival (OS) was extracted. Furthermore, information on number of cases along with median values of mRNA expression levels, hazard ratios (HR) with 95% CIs and P values were extracted from the KM plotter webpage and considered significant having P values 0.05.

GEO datasets analysis, Microarray data analysis and Gene signature definition

The mRNA expression profiling of all the samples in this study were performed on the Human Affymetrix Human Genome U133 Plus 2.0 Array or Illumina Genome Analyzer II. GSE9195 was used to show the association between FEN1 expression and tamoxifen efficacy, and DFS was analysed (35). GSE25710 was used to obtain ER α ChIP-Seq data, and the map of ER binding at whole genome level was analysed (36).

Microarray technology was utilized to investigate changes in mRNA profiles with FEN1 siRNA versus control group in MCF-7 cells. Total RNA was extracted using TRIzol[®] reagent (Invitrogen; Thermo Fisher Scientific, Inc.) and

Table 1 Clinicopathological characteristics of 65 patients with oestrogen receptor positive breast cancer

Characteristics	Cases (%)
Age (year)	
<50	39 (60.0)
≥50	26 (40.0)
Histological grade	
I, II	44 (67.7)
III	13 (20.0)
None	8 (12.3)
Tumor size (cm)	
≤2	28 (43.1)
>2	37 (56.9)
pN stage	
N0	24 (36.9)
N1+2+3	41 (63.1)
PR	
Negative	10 (15.4)
Positive	55 (84.6)
HER-2	
Negative	49 (75.4)
Positive	16 (24.6)

HER-2 positive: IHC3+ or IHC2+, HER2 FISH amplification. PR, progesterone receptor; HER-2, human epidermal growth factor receptor 2.

the RNA was purified, amplified, labeled, and hybridized according to the manufacturer's protocol (Genechem Company, Shanghai, China). Further data analysis was performed with the R software package, such as limma package. FEN1 with an expression fold change > |1.5| was considered to be statistically significantly differentially expressed. Based on the differentially expressed genes (DEGs), Gene Set Enrichment Analysis (GSEA) was performed with molecular signatures database (MSigDB) for pathways analysis (37,38).

Unsupervised hierarchical cluster analysis of genes that were changed when MCF-7 was treated with E2 (E2 *vs.* Veh.) or E2 plus 4-OHT (E2+ 4-OHT *vs.* E2) using GSE25316 dataset compared to genes that were differentially expressed upon FEN1. Genes that were

shared between ER α -dependent core genes and FEN1-regulated ones were identified as the signature genes that are controlled by both FEN1 and ER α signaling. The gene signatures were determined to coregulate by FEN1 and ER α signaling according to the ER α -dependent core genes, which were defined by changed upon E2 stimulation and transcription start site of ER α binding peak (39).

Patient tissue specimens and immunohistochemistry (IHC)

This study retrospectively analyzed 65 patients with ER+ breast cancer. These patients were admitted to the First Affiliated Hospital of China Medical University from 2002 to 2008, and had the end of five-year tamoxifen treatment or developed relapse under regular adjuvant hormone therapy (tamoxifen 20 mg/d). Clinical pathological data of the cohorts are shown in *Table 1*. Patient cohorts for IHC staining, tumor specimen collection, survey data, and all clinical and pathologic information were reviewed and approved by the Ethics Committee of China Medical University. The current study includes follow-up data available as of October 31, 2019, the median follow-up time was 152 months. The relapse-free survival (RFS) was set on the period from the date of surgery to recurrence. The overall survival (OS) was set on the period from the date of surgery to death or to the most recent clinic visit. Antibody used for IHC: Mouse Anti-Human FEN1 (working concentrations were 1:200) were purchased from Santa Cruz Biotechnology (CA, USA). The results of IHC were assessed with double-blind method, the staining results were reviewed and approved by two specialists in Department of Pathology in the first hospital of China Medical University. The positive staining of FEN1 was defined as those showing nuclei or cytoplasmic staining of tumor cells. Briefly, the scoring method that takes both staining intensity and proportion of stained cells into account. The staining intensity was classified into four categories according to the color of immune reactions: negative, 0, no staining; weak, 1, light brown; moderate, 2, brown in color; and strong, 3, with dark brown staining. The proportion of positively stained cells was reported as: 0–25%, 1; 26–50%, 2; 51–75%, 3; and 76–100%, 4. The overall expression level of FEN1 was obtained by the staining intensity and the proportion of positively stained cells. A median expression score of 6 was taken as the cut-off value, samples with scores of 0–4 were considered as low expressing, others with scores of 6–12 were defined as high expressing.

Cell culture, small interfering RNA (siRNA) transfection and lentiviral transfection

The human ER+ breast cancer cell line MCF-7 and T47D were obtained from the Type Culture Collection of the Chinese Academy of Sciences (Shanghai, China). Both cell lines were cultured in DMEM (GIBCO BRL, Grand Island, NY) containing 10% fetal bovine serum (GIBCO BRL), 100 U/mL penicillin and 100 µg/mL streptomycin in a humidified incubator at 37 °C with an atmosphere of 5% CO₂.

Small interfering RNAs (siRNAs) for FEN1 ordered from RiboBio Company (Guangzhou, China). The target sequence of FEN1 was 5'-GGGTCAAGAGGCTGAGTAA-3' (sense), 5'-UUACUCAGCCUCUUGACCCdTdT-3' (anti-sense), and negative control: 5'-UUCUCCGAACGUGUCACGUt-3' (sense), 5'-ACGUGACACGUUCGGAGAA-3' (anti-sense). The siRNAs (100 nM) were transfected into cells using Lipofectamine 2000 (Invitrogen) according to the manufacturer's instructions. Seventy-two hours after transfection, cells were harvested for the subsequent experiments.

FEN1 overexpressing and FEN1 knockdown lentivirus were purchased from Genechem Company (Shanghai, China). The processes of lentivirus transfection were performed as described previously (21). In brief, the lentiviral vectors LV-GFP-FEN1-RNAi, LV-GFP-FEN1-3FLAG and empty vector controls were synthesized (Genechem Company). The target sequence of FEN1 was the same as siRNA. To estimate transfection efficiency, our experiments utilize LV-GFP-FEN1-RNAi, LV-GFP-FEN1-3FLAG and LV-GFP-NC in which GFP is expressed as a fusion. The percent of GFP-positive cells was determined by fluorescent microscopy (BX61, Olympus, Japan) 120 hours after transfection. Poor transfection can result in low translocation efficiency. Western blot analysis was performed to detect the knock-down and overexpression efficiency.

Cell viability assay and colony formation experiments

MTT assay was used to measure the cell viability after using tamoxifen. Cells were inoculated in the 96-well plate, 5,000 cells per well. Incubation for 24 hours to make sure all cells were attached. After 96 h treatment, MTT was added to incubate for 4 h, and then dimethyl sulfoxide (DMSO) was added. OD value of the survival cells were determined under 570 nm wavelength using microplate reader (Bio-Tek, GA, USA). The percentage of cell viability was calculated. 4-OHT was purchased from Sigma-Aldrich (Merck, China).

As for colony formation assay, 1,000 cells were inoculated in 24-well plates, then cells were treated with 1 µM 4-OHT and maintained in an incubator of 5% CO₂ at 37 °C for 14 days. The culture medium was changed every three days. At the end of the experiments, cells were washed with PBS and fixed with 75% ethanol for 5 min at room temperature and then stained with Giemsa for 30 min at room temperature. Colonies with more than 50 cells were counted under an inverted microscope.

Western blot analysis

For western blot, the process was described previously (40). The membrane was incubated with the indicated primary and secondary antibodies, and the proteins were visualized by an enhanced ECL kit (Beyotime, China). Antibody: FEN1 (Genetex), ERα (Santa Cruz Biotechnology), phosphorylated(p)-ER (Cell Signaling Technology, Danvers, MA, USA), Cyclin D1 (Santa Cruz Biotechnology), Rb (Santa Cruz Biotechnology), p-Rb (Santa Cruz Biotechnology), E2F (Santa Cruz Biotechnology), Cyclin B (Santa Cruz Biotechnology), Cyclin E (Santa Cruz Biotechnology) and GAPDH (Cell Signaling Technology, Danvers, MA, USA). Imaging Densitometer with Molecular Analyst Software (Bio-Rad) and expressed as the ratios to the density of GAPDH bands.

Statistical analysis

Each experiment was repeated at least 3 times unless otherwise specified. Group data comparisons were conducted by χ^2 tests. The results were expressed as mean \pm standard deviation (SD) in this study. Associations between FEN1 expression and clinical parameters were evaluated using Chi-square test analysis. The KM method, two-tailed log-rank test, and Cox proportional hazard model were used for survival analysis. $P < 0.05$ is considered to be statistically significant. All statistical tests were performed on SPSS 20.0 software.

Results

High expression of FEN1 correlated with worse prognosis in ER+ breast cancer patients receiving tamoxifen treatment

To investigate the clinical relevance of FEN1 in ER+ breast cancer, we first correlated the mRNA expression levels of FEN1 with the RFS and OS using a KM plotter.

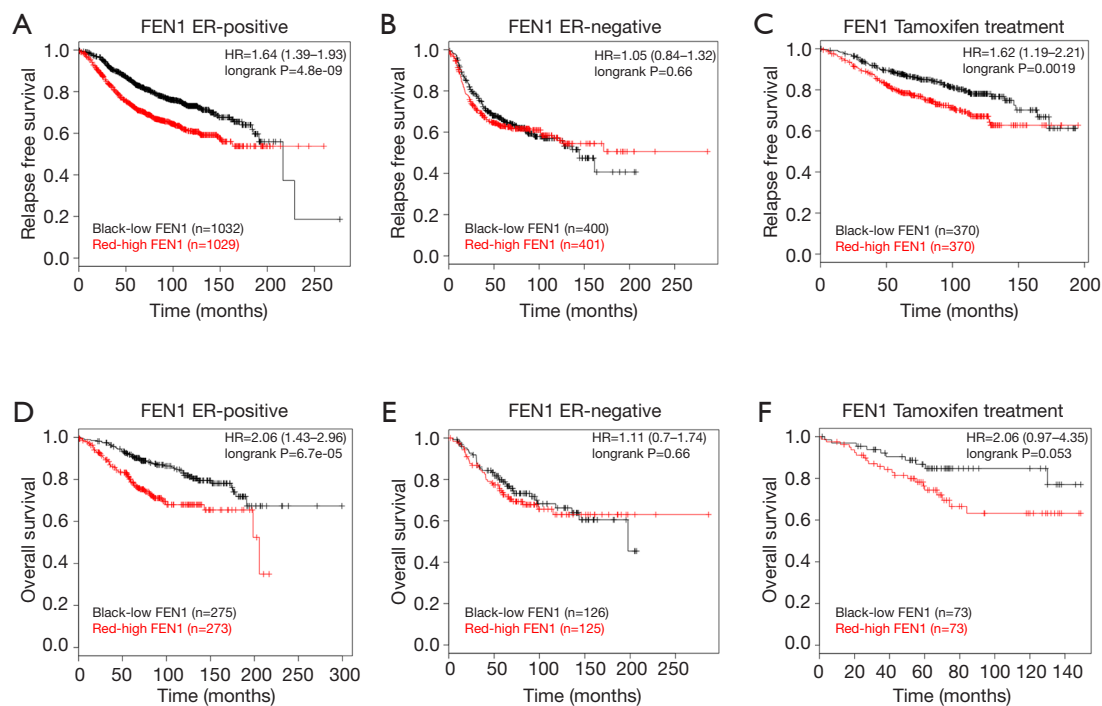


Figure 1 Determination of prognostic value of FEN1 mRNA expression using a KM plotter on-line tool: <https://kmplot.com/>. Kaplan-Meier curves of RFS in ER+ breast cancer (A), ER- breast cancer (B) and ER+ breast cancer accepted with tamoxifen treatment (C). Kaplan-Meier curves of OS in ER+ breast cancer (D), ER- breast cancer (E), and ER+ breast cancer accepted with tamoxifen treatment (F). P values were calculated by using the log-rank test. RFS, relapse-free survival; ER+, oestrogen receptor-positive; ER-, oestrogen receptor-negative; OS, overall survival.

The results showed that the high expression of FEN1 was associated with a shorter RFS for patients with ER+ breast cancer [Figure 1A, Hazard ratio (HR) = 1.64 (1.39–1.93); logrank $P=4.8 \times 10^{-9}$]. However, FEN1 expression was not prognostic in ER- breast cancers [Figure 1B; HR = 1.05 (0.84–1.32); logrank $P=0.66$]. Further, the correlation of FEN1 expression in tamoxifen-treated ER+ patients was assessed. A high expression of FEN1 correlated with a shorter RFS in the ER+ breast cancer patients who received tamoxifen [Figure 1C; HR = 1.62 (1.19–2.21); logrank $P=0.0019$]. The results of OS were consistent with the RFS (Figure 1D,E,F). Taken together, the above results suggest that FEN1 may play an important role in predicting the prognosis of patients with ER+ breast cancer and patients who received tamoxifen treatment.

Patients with high expression of FEN1 showed tamoxifen resistance

We re-analysed ER+ breast cancer patients from GSE9195

dataset, in which the patients received tamoxifen as an adjuvant treatment. There was a significant increase of FEN1 mRNA level in patients that were resistant to tamoxifen compared to the sensitive group (Figure 2A; $P=0.0062$).

Among the 65 cancer specimens in the current study, 32 patients (49.23%) demonstrated high FEN1 expression. High expression of FEN1 was significantly correlated with lymph node positivity ($P=0.013$), but not with age ($P=0.265$), histological grade ($P=0.431$) and tumor size ($P=0.162$) (Table 2). The high expression staining of FEN1 was 33.3% in disease-free patients, 87.5% in less than 2-year recurrence patients and 73.3% in more than 2-year recurrence patients (Figure 2B,C). IHC staining showed that the expression of FEN1 was significantly increased in the less than 2-year recurrent tamoxifen-resistant tumours than that in tamoxifen-sensitive tumours (recurrence-free and more than 2-year recurrence); high FEN1 expression was associated with poor prognosis in breast cancer patients receiving tamoxifen therapy (DFS, Figure 2D, $P<0.001$; OS,

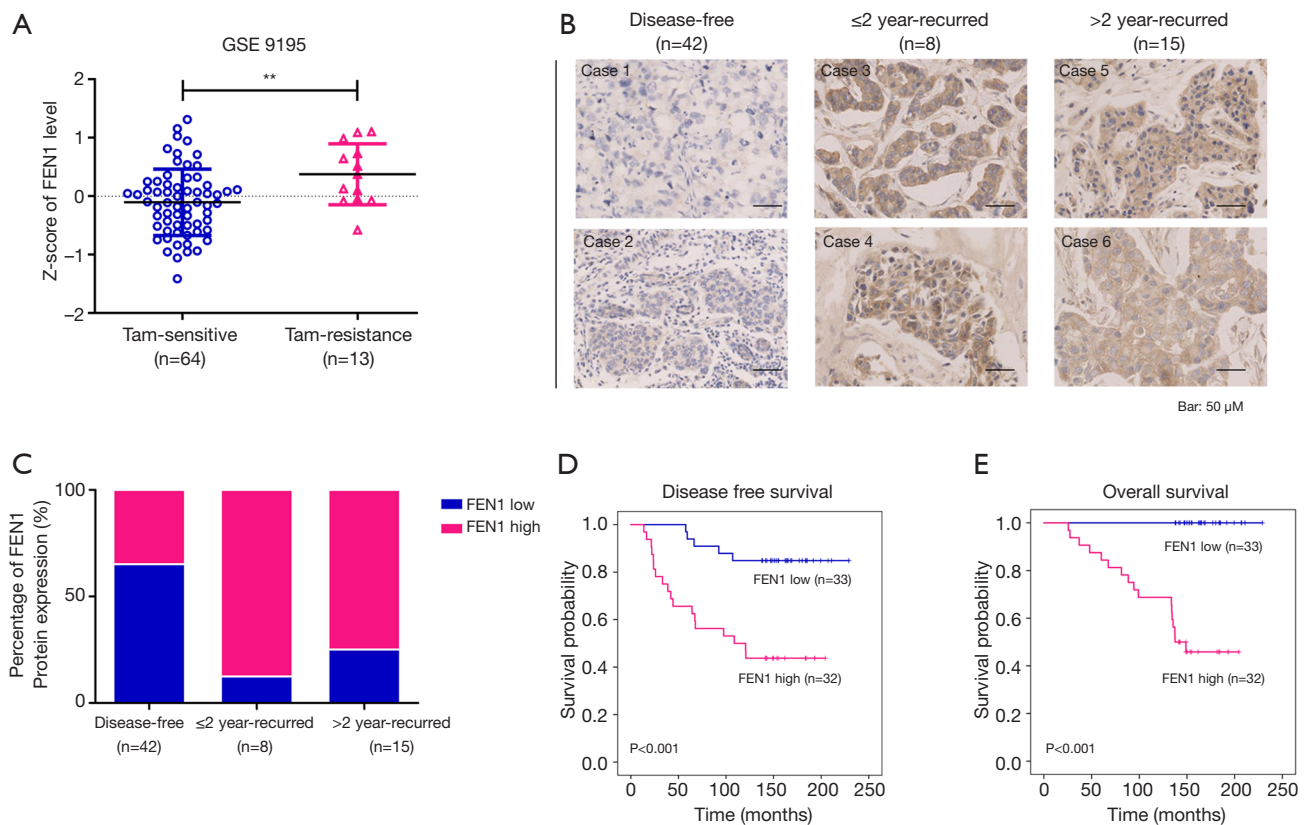


Figure 2 FEN1 expression increases during the development of tamoxifen resistance in patients with breast cancer. (A) Kaplan-Meier analysis of disease-free survival based on FEN1 mRNA levels using the GSE9195 cohort including a tamoxifen-resistant (Tam-R) group and tamoxifen-sensitive (Tam-S) group. (B) Representative IHC images of FEN1 protein in disease-free, less than 2-year recurrence and more than 2-year recurrence breast cancer tissues. Scale bars: 50 μm. (C) Bar graph showing the proportion of high expression of FEN1 in ER+ breast cancer tissues with disease-free, less than 2-year recurrence and more than 2-year recurrence. Kaplan-Meier analysis of DFS (D) or OS (E) curves for patients with tamoxifen-treated ER+ breast cancer with low FEN1 expression versus high FEN1 expression. P-values were determined by log-rank test. IHC, immunohistochemistry; DFS, disease-free survival; OS, overall survival.

Figure 2E, $P < 0.001$).

Univariate and multivariate analysis for PFS and OS

Furthermore, the univariate and a Cox multivariable proportional hazard model were constructed to evaluate independent prognostic significance of FEN1 expression and some clinicopathological characteristics. Univariate regression analysis showed that FEN1 expression ($P = 0.001$) and tumor size ($P = 0.024$) were significantly associated with DFS in 65 patients with ER positive BC (Table 3). These variables with $P < 0.10$ were included in multivariate regression analysis using a forward step-wise method. The results showed that FEN1 expression ($P = 0.001$) and tumor size ($P = 0.023$) were independent factors for DFS. We next

assessed whether these variables had the prognostic impacts on OS as well. Multivariable analysis of outcomes for the entire cohort showed that FEN1 expression ($P = 0.025$) and tumor size ($P = 0.011$) were significantly associated with worse survival (Table 4). Since equation does not converge, HR and CIs was not available.

FEN1 rendered tamoxifen resistance in ER-positive breast cancer cell lines

To explore further the actual function of FEN1 in tamoxifen resistance, we over-expressed or knocked-down FEN1 in MCF-7 and T47D cell lines (Figure 3A,B,C), and then measured cellular response to increasing concentrations of 4-hydroxytamoxifen (4-OHT), the active metabolite of

Table 2 Relationship between the expression of FEN1 and clinicopathological characteristics in 65 patients with ER positive breast cancer accepted with tamoxifen therapy

Characteristics	Cases	FEN1 expression		P value
		Low (%)	High (%)	
Age (year), median (range)				0.265
<50	39	22 (56.4)	17 (43.6)	
≥50	26	11 (42.3)	15 (57.7)	
Histological grade				0.602
I, II	44	20 (45.5)	24 (54.5)	
III	13	7 (53.8)	6 (46.2)	
NA	8	6 (75.0)	2 (25.0)	
Tumor size (cm)				0.163
≤2	28	17 (60.7)	11 (39.3)	
>2	37	16 (43.2)	21 (56.8)	
pN stage				0.013*
N0	24	17 (70.8)	7 (29.2)	
N1+2+3	41	16 (39.0)	25 (61.0)	

The categorical parameters were compared with the χ^2 -test or Fisher's exact test and analysis of variance as appropriate. *, P<0.05. FEN1, Flap endonuclease-1; ER, oestrogen receptor.

Table 3 Univariate and multivariate analysis of DFS in 65 patients with ER positive breast cancer

Characteristic	Univariate analysis			Multivariate analysis		
	HR	95% CI	P	HR	95% CI	P
FEN1 expression	5.15	1.91–13.90	0.001*	5.36	1.97–14.58	0.001*
Age (year)	0.71	0.30–1.67	0.433			
Histological grade	1.67	0.69–4.05	0.26			
Tumor size	2.39	1.12–5.10	0.024*	2.75	1.15–6.58	0.023*
pN stage	1.73	0.68–4.38	0.25			
PR	0.69	0.25–1.84	0.45			
HER-2	1.55	0.57–4.17	0.39			

*, P<0.05. DFS, disease-free survival; FEN1, Flap endonuclease-1; ER, oestrogen receptor; HR, hazard ratio; PR, progesterone receptor; HER-2, human epidermal growth factor receptor 2; HER-2 positive (IHC3+ or IHC2+, HER2 FISH amplification).

tamoxifen. After over-expression of FEN1, MCF-7 and T47D demonstrated a decreased sensitivity to tamoxifen, but we observed an inhibitory effect of tamoxifen on MCF-7 and T47D cell proliferation after deletion of FEN1 (Figure 3D,E,F). Combining the above, these results indicated that FEN1 plays an essential role in driving tamoxifen resistance and may act as a promising therapeutic target.

FEN1 over-expression elicited an Endo-R gene signature and ER/Cyclin D/Rb axis

The better to understand the effects of FEN1 in tamoxifen resistance, the RNA-seq analysis revealed a total of 271 up-regulated genes and 336 down-regulated genes (FC >1.5, P<0.05) in si-FEN1 MCF-7 cells compared to the control

Table 4 Univariate analysis of OS in 65 patients with ER positive breast cancer

Characteristic	Univariate analysis		
	HR	95% CI	P
FEN1 expression	Nofit	Nofit	0.025*
Age (year)	0.81	0.30–2.19	0.68
Histological grade	1.42	0.50–4.02	0.52
Tumor size	3.27	1.31–8.18	0.011*
pN stage	2.88	0.83–10.03	0.09
PR	0.64	0.21–1.95	0.43
HER-2	1.66	0.54–5.08	0.38

*, P<0.05. HER-2 positive: IHC3+ or IHC2+, HER2 FISH amplification. OS, overall survival; ER, oestrogen receptor; HR, hazard ratio; FEN1, Flap endonuclease-1; PR, progesterone receptor; HER-2, human epidermal growth factor receptor 2.

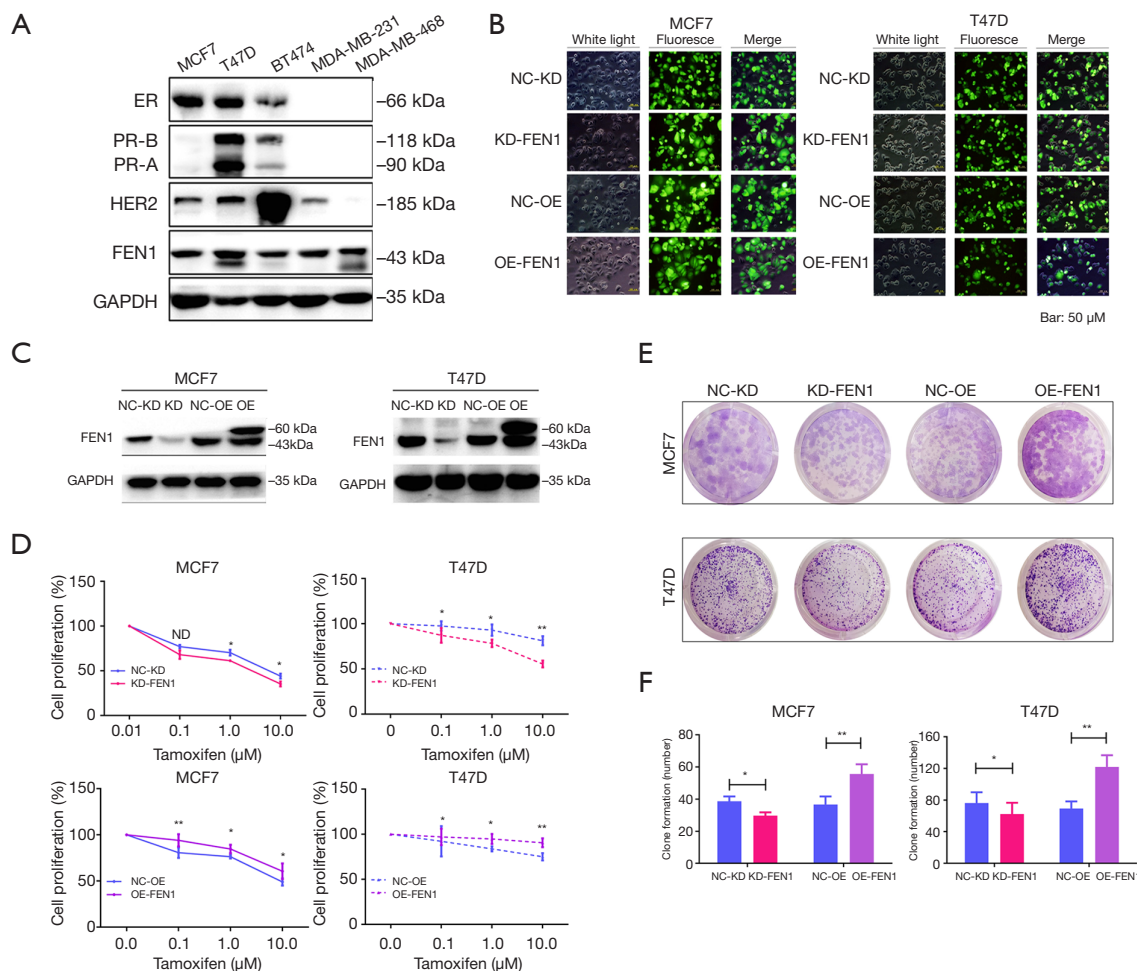


Figure 3 FEN1 confers tamoxifen resistance in ER-positive breast cancer cells. (A) Comparison of FEN1 protein levels in different breast cancer cell lines. Detection of the efficiency of lentiviral transfection in MCF-7 and T47D using florescent microscopy (B) and western blot assay (C). Cell viability to tamoxifen by MTT (D) and colony formation experiments (E) in MCF-7 and T47D cell lines upon over-expressing or knocking-down either one empty vector or the other (stained with Giemsa for 30 min at room temperature). (F) P values were calculated by two-tailed *t*-test. *, P<0.05; **, P<0.01.

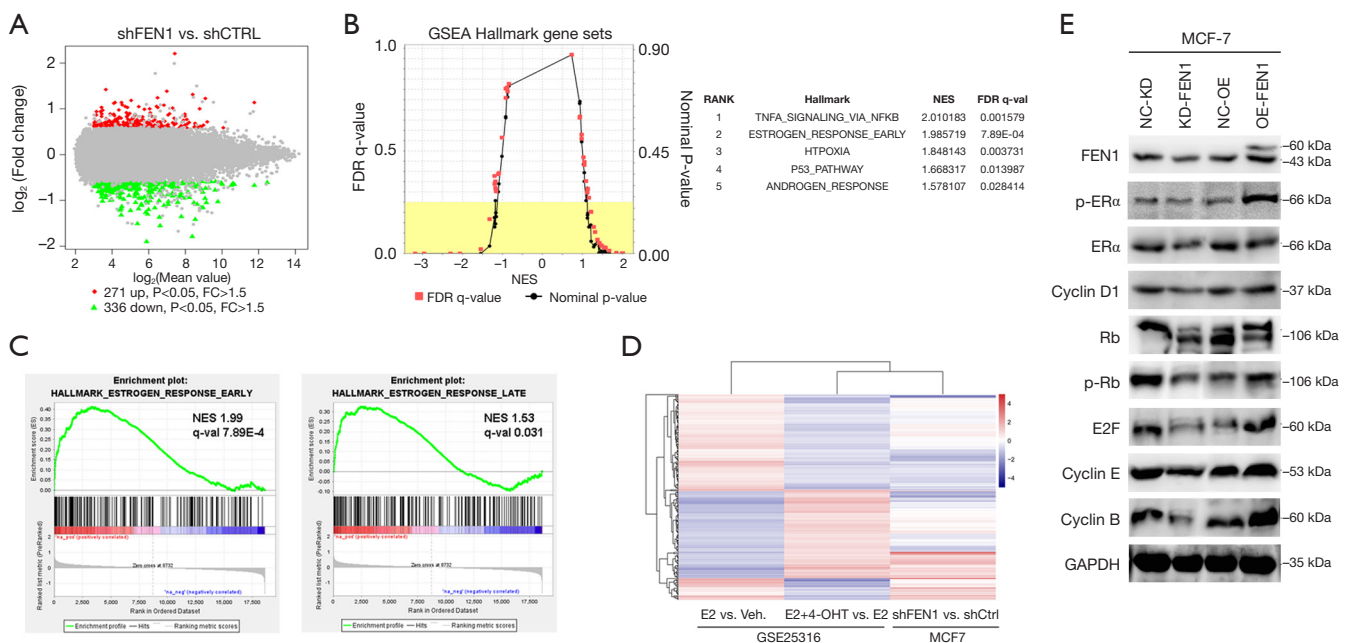


Figure 4 FEN1 regulates an ER-associated transcriptional profile in favour of endocrine resistance. (A) Volcano map of the 607 differentially expressed genes between shFEN1 and control in MCF-7 cell line. (B) Plot of false discovery rate (FDR) versus the normalised enrichment score (NES) based upon GSEA from microarray data. The top five ranked positively enriched gene sets are shown on the right. (C) GSEA of 336 genes down-regulated in shFEN1 as compared to the Hallmark “Oestrogen Response Early” Geneset and “Oestrogen Response Late” Geneset. (D) Unsupervised hierarchical cluster analysis of genes that were changed when MCF-7 was treated with E2 (E2 *versus* Veh.) or E2 plus 4-OHT (E2+ 4-OHT *versus* E2) using the GSE25316 dataset compared to genes that were differentially expressed upon FEN1 knock-down in MCF-7 cells (shFEN1 *versus* shCtrl). The colour scale bar indicates the log₂ of differential gene expression from the lowest (blue) to the highest (red) level. (E) Western blot assay was applied to determine the levels of related proteins in MCF-7 cell lines after over-expressing or knocking-down.

group (Figure 4A, Table S1). Functional annotation of these differential genes in the GSEA to interrogate the oncogenic gene signatures from the Molecular Signatures Database (MSigDB) showed that the “OESTROGEN_RESPONSE_EARLY” pathway ($P=7.89 \times 10^{-4}$) was mostly annotated according to the adjusted P value (Figure 4B). Interestingly, within the down-regulated genes, the most enriched term was “OESTROGEN RESPONSE EARLY” ($P=7.89 \times 10^{-4}$) and “OESTROGEN RESPONSE LATE” ($P=0.031$), suggesting that over-expression of FEN1 enhanced ER-related downstream signalling (Figure 4C). In addition, the FEN1-induced mRNA profile was in agree with the Endo-R Gene Signature that was up-regulated in the E2-stimulated cases and ran contrary to tamoxifen inhibition (Figure 4D). These data suggested that the high expression of FEN1 potentially drives a transcriptional programme associated with high ER signalling that contributes to endocrine resistance. To confirm the above analysis, we

knocked-down and over-expressed FEN1 respectively. As shown in Figure 4E, p-ERα, cyclin D1, and p-Rb were up-regulated after FEN1 over-expression, and vice versa. We may thus infer that over-expression of FEN1 activates the ERα/cyclin D1/Rb axis.

Discussion

For more than four decades, tamoxifen has been used to treat ER+ breast cancer as a classic medicine for endocrine therapy; however, a proportion of patients with ER+ breast cancer that received tamoxifen treatment eventually acquired resistance thereto (6,7). The major challenge is identifying new therapeutic targets or specific biomarkers that are predictive of the therapeutic responses to endocrine therapy to achieve successful treatment. A study has highlighted a correlation between FEN1 over-expression and poor prognosis in breast cancer (31). In this study, our

results showed that elevated FEN1 mRNA expressions were correlated with shorter RFS, DMFS, and OS in breast cancer patients, and more significant in ER-positive breast cancer and tamoxifen treatment failure subtype. Next, the IHC analysis of FEN1 protein levels in 55 ER+ breast cancer patients also demonstrated that high expression of FEN1 protein was highly significantly associated with shorter DFS and OS in tamoxifen treatment. Our results showed that the FEN1 is an important prognostic biomarker of breast cancer patients, especially in the tamoxifen treatment failure group. The above results showed that FEN1 may be a biomarker of tamoxifen resistance. The in-depth study of the function and mechanism of FEN1 participation in tamoxifen resistance plays an important role in screening the benefit to patients of tamoxifen and reversing drug resistance.

In recent years, studies have reported that the high expression of FEN1 is involved in drug resistance processes such as chemotherapies, radiation treatment, and targeted therapy (24-26). Through inhibiting expression of FEN1 or application of FEN1 small molecule inhibitors, it can reverse drug resistance and synergistic chemotherapy/radiotherapy sensitivity (26,41-47). These results indicated that FEN1 is a key molecule associated with the resistance to anti-cancer therapy, however, the precise functions of FEN1 in tamoxifen-resistance remain unknown. The further to confirm this ability, we established FEN1 over-expressed and knocked-down ER+ breast cancer cell lines. Next, both MTT experiments and colony formation experiments showed that tamoxifen-sensitive breast cancer cell lines MCF-7 and T47D were less sensitive to tamoxifen after FEN1 was over-expressed, and the inhibitory effect of tamoxifen on the growth of breast cancer cells was enhanced by knocking out the FEN1 gene. These results indicated that breast cancer cell over-expressed FEN1 is resistant to tamoxifen and knocking out FEN1 would enhance the inhibitory effect of tamoxifen on cells. A high expression of FEN1 was related to drug resistance, and it was significant to reversing drug resistance, especially tamoxifen resistance caused by over-expression of FEN1.

Previous findings have indicated that FEN1 may active EGFR signalling, and promote epithelial-mesenchymal transition (EMT) and anti-apoptosis, which are the classic mechanism of endocrine resistance (21,48,49). Schultz-Norton *et al.* found that oestrogen promotes the binding of FEN1 to multiple domains of ER α , including the DNA domain, C-terminal, and carboxy-terminal domains, thereby enhancing ER α -mediated oestrogen-responsive

gene transcription (33). Moreover, the study from our team has reported that FEN1 may mediate trastuzumab resistance *via* enhancing ER α -target gene transcription (24). The abnormal activation of ER α -target gene transcription was another mechanism of tamoxifen resistance (50). These previous studies have provided several underlying molecular mechanisms of tamoxifen resistance caused by FEN1. To find the reason, we performed GSEA using the MSigDB hallmark gene sets, which indicated two hallmark gene sets (“oestrogen response early” and “oestrogen response late”) were positively correlated with FEN1 expression. Further verification through western blot assay showed that FEN1 over-expression could significantly increase the level of p-ER α , cyclin D1, p-RbSer807/811, and E2F to initiate transcription of downstream target genes such as cyclin E and cyclin B, suggesting that the promotion of Rb phosphorylation was probably involved in FEN1-induced tamoxifen resistance. This was consistent with earlier studies reporting that FEN1 enhances ER α -mediated oestrogen-responsive gene transcription (33). From these results, we proposed that FEN1 stimulated the activation of the ER α /cyclinD1/Rb axis to promote tamoxifen resistance. However, this study had the some limitations of retrospective studies conducted at a single-center and smaller sample size. Therefore, the findings require validation with large-scale, multi-center clinical studies.

Conclusions

In summary, our study confirmed that the high expression of FEN1 was related to poor survival in ER+ breast cancer patients. We found that breast cancer cells were less sensitive to tamoxifen after FEN1 was over-expressed and became sensitive to tamoxifen when FEN1 was knocked out. For the first time we found that FEN1 may participate in tamoxifen resistance *via* the ER α /Cyclin D1/Rb axis, which provided evidence that may improve precision treatment with tamoxifen. In future, whether inhibition of FEN1 may reverse tamoxifen resistance (or not) warrants further investigation.

Acknowledgments

Funding: This work was supported by National Natural Science Foundation of China (No. 81672605); National Science and Technology Major Project of the Ministry of Science and Technology of China (No. 2017ZX09304025);

The Key Research and Development Program of Liaoning Province(2018225060); Special Project of Liaoning Province of China (2019020176-JH1/103); Science and Technology Plan Project of Liaoning Province (No. 2013225585); Technological The general project of Liaoning province department of education (No. L2015588); Science and Technology Plan Project of Liaoning Province (No. 2015020458); National Key R&D Program of China (Grant #2018YFC1311600).

Footnote

Reporting Checklist: The authors have completed the REMARK reporting checklist. Available at <http://dx.doi.org/10.21037/atm-20-3068>

Peer Review File: Available at <http://dx.doi.org/10.21037/atm-20-3068>

Conflicts of Interest: All authors have completed the ICMJE uniform disclosure form (available at <http://dx.doi.org/10.21037/atm-20-3068>). The authors have no conflicts of interest to declare.

Ethical Statement: The authors are accountable for all aspects of the work in ensuring that questions related to the accuracy or integrity of any part of the work are appropriately investigated and resolved. The study was conducted in accordance with the Declaration of Helsinki (as revised in 2013). The study was approved by institutional/regional/national ethics/committee/ethics board of the first hospital of China Medical University (No. [2016]120: the registration number of ethics board) and informed consent was taken from all the patients.

Open Access Statement: This is an Open Access article distributed in accordance with the Creative Commons Attribution-NonCommercial-NoDerivs 4.0 International License (CC BY-NC-ND 4.0), which permits the non-commercial replication and distribution of the article with the strict proviso that no changes or edits are made and the original work is properly cited (including links to both the formal publication through the relevant DOI and the license). See: <https://creativecommons.org/licenses/by-nc-nd/4.0/>.

References

1. Bray F, Ferlay J, Soerjomataram I, et al. Global cancer statistics 2018: GLOBOCAN estimates of incidence and mortality worldwide for 36 cancers in 185 countries. *CA Cancer J Clin* 2018;68:394-424.
2. Harbeck N, Gnant M. Breast cancer. *Lancet* 2017;389:1134-50.
3. Dobovišek L, Krstanović F, Borštnar S, et al. Cannabinoids and Hormone Receptor-Positive Breast Cancer Treatment. *Cancers (Basel)* 2020;12:525.
4. Waks AG, Winer EP. Breast Cancer Treatment: A Review. *JAMA* 2019;321:288-300.
5. Ruddy KJ, Ganz PA. Treatment of Nonmetastatic Breast Cancer. *JAMA* 2019;321:1716-7.
6. Musgrove EA, Sutherland RL. Biological determinants of endocrine resistance in breast cancer. *Nat Rev Cancer* 2009;9:631-43.
7. Jordan VC, O'Malley BW. Selective estrogen-receptor modulators and antihormonal resistance in breast cancer. *J Clin Oncol* 2007;25:5815-24.
8. Schultz-Norton JR, Ziegler YS, Nardulli AM. ERalpha-associated protein networks. *Trends Endocrinol Metab* 2011;22:124-9.
9. Ratanaphan A. A DNA repair BRCA1 estrogen receptor and targeted therapy in breast cancer. *Int J Mol Sci* 2012;13:14898-916.
10. Zheng L, Jia J, Finger LD, et al. Functional regulation of FEN1 nuclease and its link to cancer. *Nucleic Acids Res* 2011;39:781-94.
11. Singh P, Zheng L, Chavez V, et al. Concerted action of exonuclease and Gap-dependent endonuclease activities of FEN-1 contributes to the resolution of triplet repeat sequences (CTG)_n- and (GAA)_n-derived secondary structures formed during maturation of Okazaki fragments. *J Biol Chem* 2007;282:3465-77.
12. Liu P, Qian L, Sung JS, et al. Removal of oxidative DNA damage via FEN1-dependent long-patch base excision repair in human cell mitochondria. *Mol Cell Biol* 2008;28:4975-87.
13. Saharia A, Stewart SA. FEN1 contributes to telomere stability in ALT-positive tumor cells. *Oncogene* 2009;28:1162-7.
14. Sampathi S, Bhusari A, Shen B, et al. Human flap endonuclease I is in complex with telomerase and is required for telomerase-mediated telomere maintenance. *J Biol Chem* 2009;284:3682-90.
15. Zheng L, Zhou M, Chai Q, et al. Novel function of the flap endonuclease 1 complex in processing stalled DNA replication forks. *EMBO Rep* 2005;6:83-9.
16. Parrish JZ, Yang C, Shen B, et al. CRN-1, a

- Caenorhabditis elegans FEN-1 homologue, cooperates with CPS-6/EndoG to promote apoptotic DNA degradation. *EMBO J* 2003;22:3451-60.
17. Zheng L, Dai H, Zhou M, et al. Fen1 mutations result in autoimmunity, chronic inflammation and cancers. *Nat Med* 2007;13:812-9.
 18. Larsen E, Gran C, Saether BE, et al. Proliferation failure and gamma radiation sensitivity of Fen1 null mutant mice at the blastocyst stage. *Mol Cell Biol* 2003;23:5346-53.
 19. Illuzzi JL, Wilson DM 3rd. Base excision repair: contribution to tumorigenesis and target in anticancer treatment paradigms. *Curr Med Chem* 2012;19:3922-36.
 20. Kucherlapati M, Yang K, Kuraguchi M, et al. Haploinsufficiency of Flap endonuclease (Fen1) leads to rapid tumor progression. *Proc Natl Acad Sci U S A* 2002;99:9924-9.
 21. Zeng X, Qu X, Zhao C, et al. FEN1 mediates miR-200a methylation and promotes breast cancer cell growth via MET and EGFR signaling. *FASEB J* 2019;33:10717-30.
 22. Zhang K, Keymeulen S, Nelson R, et al. Overexpression of Flap Endonuclease 1 Correlates with Enhanced Proliferation and Poor Prognosis of Non-Small-Cell Lung Cancer. *Am J Pathol* 2018;188:242-51.
 23. He L, Zhang Y, Sun H, et al. Targeting DNA Flap Endonuclease 1 to Impede Breast Cancer Progression. *EBioMedicine* 2016;14:32-43.
 24. Zeng X, Che X, Liu YP, et al. FEN1 knockdown improves trastuzumab sensitivity in human epidermal growth factor 2-positive breast cancer cells. *Exp Ther Med* 2017;14:3265-72.
 25. He L, Luo L, Zhu H, et al. FEN1 promotes tumor progression and confers cisplatin resistance in non-small-cell lung cancer. *Mol Oncol* 2017;11:640-54.
 26. Ward TA, McHugh PJ, Durant ST. Small molecule inhibitors uncover synthetic genetic interactions of human flap endonuclease 1 (FEN1) with DNA damage response genes. *PLoS One* 2017;12:e0179278.
 27. Lam JS, Seligson DB, Yu H, et al. Flap endonuclease 1 is overexpressed in prostate cancer and is associated with a high Gleason score. *BJU Int* 2006;98:445-51.
 28. Nikolova T, Christmann M, Kaina B. FEN1 is overexpressed in testis, lung and brain tumors. *Anticancer Res* 2009;29:2453-9.
 29. Singh P, Yang M, Dai H, et al. Overexpression and hypomethylation of flap endonuclease 1 gene in breast and other cancers. *Mol Cancer Res* 2008;6:1710-7.
 30. Sato M, Girard L, Sekine I, et al. Increased expression and no mutation of the Flap endonuclease (FEN1) gene in human lung cancer. *Oncogene* 2003;22:7243-6.
 31. Abdel-Fatah TM, Russell R, Albarakati N, et al. Genomic and protein expression analysis reveals flap endonuclease 1 (FEN1) as a key biomarker in breast and ovarian cancer. *Mol Oncol* 2014;8:1326-38.
 32. Wang J, Zhou L, Li Z, et al. YY1 suppresses FEN1 overexpression and drug resistance in breast cancer. *BMC Cancer* 2015;15:50.
 33. Schultz-Norton JR, Walt KA, Ziegler YS, et al. The deoxyribonucleic acid repair protein flap endonuclease-1 modulates estrogen-responsive gene expression. *Mol Endocrinol* 2007;21:1569-80.
 34. Györfy B, Lanczky A, Eklund AC, et al. An online survival analysis tool to rapidly assess the effect of 22,277 genes on breast cancer prognosis using microarray data of 1,809 patients. *Breast Cancer Res Treat* 2010;123:725-31.
 35. Loi S, Haibe-Kains B, Desmedt C, et al. Predicting prognosis using molecular profiling in estrogen receptor-positive breast cancer treated with tamoxifen. *BMC Genomics* 2008;9:239.
 36. Hurtado A, Holmes KA, Ross-Innes CS, et al. FOXA1 is a key determinant of estrogen receptor function and endocrine response. *Nat Genet* 2011;43:27-33.
 37. Mootha VK, Lindgren CM, Eriksson KF, et al. PGC-1alpha-responsive genes involved in oxidative phosphorylation are coordinately downregulated in human diabetes. *Nat Genet* 2003;34:267-73.
 38. Subramanian A, Tamayo P, Mootha VK, et al. Gene set enrichment analysis: a knowledge-based approach for interpreting genome-wide expression profiles. *Proc Natl Acad Sci U S A* 2005;102:15545-50.
 39. Zhang Y, Liu T, Meyer CA, et al. Model-based analysis of ChIP-Seq (MACS). *Genome Biol* 2008;9:R137.
 40. Li H, Xu L, Li C, et al. Ubiquitin ligase Cbl-b represses IGF-I-induced epithelial mesenchymal transition via ZEB2 and microRNA-200c regulation in gastric cancer cells. *Mol Cancer* 2014;13:136.
 41. Mileo AM, Di Venere D, Mardente S, et al. Artichoke Polyphenols Sensitize Human Breast Cancer Cells to Chemotherapeutic Drugs via a ROS-Mediated Downregulation of Flap Endonuclease 1. *Oxid Med Cell Longev* 2020;2020:7965435.
 42. Dong S, Xiao Y, Ma X, et al. miR-193b Increases the Chemosensitivity of Osteosarcoma Cells by Promoting FEN1-Mediated Autophagy. *Onco Targets Ther* 2019;12:10089-98.
 43. Li JL, Wang JP, Chang H, et al. FEN1 inhibitor increases sensitivity of radiotherapy in cervical cancer cells. *Cancer*

- Med 2019;8:7774-80.
44. Zhu H, Wu C, Wu T, et al. Inhibition of AKT Sensitizes Cancer Cells to Antineoplastic Drugs by Downregulating Flap Endonuclease 1. *Mol Cancer Ther* 2019;18:2407-20.
 45. Wang Y, Li S, Zhu L, et al. Letrozole improves the sensitivity of breast cancer cells overexpressing aromatase to cisplatin via down-regulation of FEN1. *Clin Transl Oncol* 2019;21:1026-33.
 46. He L, Yang H, Zhou S, et al. Synergistic antitumor effect of combined paclitaxel with FEN1 inhibitor in cervical cancer cells. *DNA Repair (Amst)* 2018;63:1-9.
 47. Lu X, Liu R, Wang M, et al. MicroRNA-140 impedes DNA repair by targeting FEN1 and enhances chemotherapeutic response in breast cancer. *Oncogene* 2020;39:234-47.
 48. Li C, Zhou D, Hong H, et al. TGF β 1- miR-140-5p axis mediated up-regulation of Flap Endonuclease 1 promotes epithelial-mesenchymal transition in hepatocellular carcinoma. *Aging* 2019;11:5593-612.
 49. Xie C, Wang K, Chen D. Flap endonuclease 1 silencing is associated with increasing the cisplatin sensitivity of SGC7901 gastric cancer cells. *Mol Med Rep* 2016;13:386-92.
 50. Gutierrez MC, Detre S, Johnston S, et al. Molecular changes in tamoxifen-resistant breast cancer: relationship between estrogen receptor, HER-2, and p38 mitogen-activated protein kinase. *J Clin Oncol* 2005;23:2469-76.

Cite this article as: Xu L, Shen JM, Qu JL, Song N, Che XF, Hou KZ, Shi J, Zhao L, Shi S, Liu YP, Qu XJ, Teng YE. FEN1 is a prognostic biomarker for ER+ breast cancer and associated with tamoxifen resistance through the ER α /cyclin D1/Rb axis. *Ann Transl Med* 2021;9(3):258. doi: 10.21037/atm-20-3068

Table S1 DEGs in mRNA profiles with FEN1 silenced versus control MCF7 breast cancer cells

probeSet	Fold change	Regulation	Gene Symbol
11743856_a_at	-1.6997063	down	CTHRC1
11758358_x_at	-1.7958246	down	SLC9A4
11719789_x_at	1.5218512	up	TUBB2A
11755202_a_at	1.8579235	up	VTCN1
11734124_a_at	1.6881026	up	FSTL4
11752826_a_at	1.5353385	up	RORC
11763901_s_at	1.5865077	up	SNORA63
11749929_x_at	1.5514666	up	PGPEP1
11736024_at	-1.5449198	down	MED28
11717061_a_at	-1.6919817	down	PPP1R1B
11745290_a_at	-1.5170231	down	PHTF1
11722571_at	-1.5052588	down	CCNA2
11725426_a_at	-1.7164474	down	RAB27A
11761859_a_at	-1.6736869	down	AUP1
11761735_a_at	-1.5115865	down	RXRB
11759603_at	-1.5184668	down	BCL2L13
11762610_at	-1.5178145	down	YIF1B
11742542_s_at	-1.5679233	down	OR1S2
11742542_s_at	-1.5679233	down	OR1S1
11730818_a_at	-2.0659351	down	CTDSPL2
11722870_at	-2.2668421	down	RAD1
11763901_s_at	1.5865077	up	SNORA81
11733765_at	-1.77975	down	IFNB1
11731010_x_at	-1.7451181	down	WDR89
11718395_s_at	1.5289985	up	JUN
11736893_a_at	1.6100576	up	C3orf67
11720238_at	-1.5003693	down	MAPK9
11729910_at	-1.7879158	down	DNAH11
11746142_a_at	1.6743624	up	ZNF611
11728519_a_at	1.5750706	up	ZNF79
11725912_a_at	1.7855595	up	ERBB4
11759311_a_at	1.5527245	up	IGFBPL1
11729454_x_at	-1.514477	down	CYP2B6
11752655_at	1.8229395	up	SERPINA13
11729169_a_at	1.9863935	up	DUSP10
11762901_at	1.5711468	up	C7orf55

11757086_s_at	-1.6338632	down	C17orf109
11762669_at	-1.8316946	down	MTIF3
11729345_a_at	-1.556195	down	ZNF513
11716185_a_at	1.5477759	up	ALCAM
11723060_at	1.5348724	up	RILPL2
11724691_at	1.7075255	up	RIBC2
11744445_a_at	-1.5115037	down	DUSP14
11744972_a_at	-1.6110907	down	MYO15A
11724399_a_at	-1.6495594	down	DDX60L
11719818_at	1.5865077	up	PIP
11723836_a_at	1.6276922	up	SPNS2
11730681_at	1.5174594	up	PPAPDC1B
11718152_a_at	1.5334653	up	PPFIBP2
11737353_a_at	-1.5029784	down	CDC20B
11730493_a_at	-1.5564383	down	KCNK2
11739789_a_at	-1.9680704	down	GCFC2
11736630_at	1.5484738	up	BTBD17
11715987_a_at	-1.6284701	down	GH1
11723975_x_at	-1.8165959	down	APOL3
11724879_at	1.6297055	up	ZNF217
11744434_a_at	-1.5037113	down	PARP9
11740925_a_at	1.573273	up	FAM151B
11740597_a_at	1.6284698	up	FAM161B
11744630_a_at	-1.5794997	down	NXPE3
11724762_a_at	2.1152382	up	DEPTOR
11753942_a_at	1.5205561	up	UCA1
11745376_a_at	-1.6616719	down	APOL6
11759860_at	-1.7960498	down	BACH1
11748034_a_at	2.2706246	up	CMAHP
11752557_a_at	1.6600755	up	CREBRF
11746044_a_at	1.6295907	up	ELF2
11757148_at	2.2010362	up	SNORA21
11724703_a_at	1.6207314	up	ELF5
11751548_a_at	1.5421206	up	C10orf10
11746618_a_at	1.5186651	up	RASSF8
11733283_a_at	-1.5246918	down	ZNF673
11743437_a_at	-1.5741671	down	DEM1

11718941_a_at	-1.6145281	down	LSM14B
11729459_x_at	2.1780386	up	BNIPL
11719844_at	-1.5203722	down	SMAP2
11721476_a_at	1.5930574	up	AP1S1
11721349_s_at	-1.6565567	down	USP18
11730495_s_at	-1.5617357	down	TYR
11752106_x_at	1.5223	up	CEACAM5
11739952_a_at	1.6284698	up	GFOD1
11723491_a_at	1.6295227	up	ARHGEF3
11717125_at	1.548569	up	SH3PXD2A
11736915_at	1.6055179	up	HIST1H1D
11750159_a_at	-2.0244331	down	BATF2
11735184_at	-1.5870059	down	EXOSC6
11741732_a_at	-1.7115923	down	ANP32E
11751089_a_at	-1.5804669	down	GTF2H4
11743188_a_at	1.5163038	up	KIAA1430
11736956_a_at	-2.193032	down	ZNF687
11756515_s_at	-1.7682297	down	EXOSC1
11741958_a_at	1.5039828	up	IL6R
11731152_s_at	-1.5414933	down	MTRR
11747171_a_at	1.5150193	up	MXD4
11737896_s_at	1.533185	up	TAF13
11727294_s_at	-1.5458648	down	ALG10B
11736152_a_at	1.80477	up	XPR1
11763901_s_at	1.5865077	up	EIF4A2
11732875_s_at	1.6415458	up	GAGE8
11762831_a_at	-1.7879152	down	TCHP
11752355_x_at	1.5184969	up	KIAA1217
11751706_a_at	-2.9354703	down	CLN6
11741878_a_at	-1.5732288	down	PML
11731669_at	-1.5578055	down	GPR65
11725412_s_at	-1.5380977	down	TRIM14
11740131_at	-2.239103	down	KANSL1L
11735452_at	1.5180753	up	NHLRC1
11730556_s_at	-1.6752697	down	TRIM6-TRIM34
11718964_at	1.5783736	up	NUFIP2
11719024_at	1.6125804	up	ZNF652

11738822_at	-1.5847695	down	OR9Q1
11721233_a_at	1.528376	up	ZNF75D
11740998_a_at	1.776621	up	DGKA
11752614_a_at	1.5602055	up	NUP214
11750700_a_at	-1.6967719	down	ACSL1
11762319_at	-1.7020565	down	MPDU1
11718792_a_at	1.6464344	up	EXOC4
11722420_a_at	1.6261882	up	PPP3CC
11761892_at	-1.5022238	down	LINC00334
11756514_a_at	1.5425503	up	TEKT5
11736105_at	1.5310352	up	ZNF750
11760160_at	-1.5827502	down	USP36
11747995_x_at	1.569858	up	TBC1D1
11739227_a_at	-1.8985628	down	FBXW11
11758312_x_at	1.5214931	up	TBC1D3
11751388_a_at	-3.4580607	down	FEN1
11763166_a_at	-1.6106652	down	MARS
11730357_at	1.8881047	up	KCNE4
11763226_x_at	1.5846983	up	IL8
11739985_a_at	1.5939617	up	AMACR
11715601_a_at	1.7243503	up	PPP1R11
11727256_a_at	-1.5657091	down	ZNF20
11750167_a_at	1.5824155	up	CAPN2
11751345_at	-1.5377406	down	LOC100289637
11722370_a_at	-2.8449247	down	TRIM22
11749217_a_at	1.6397165	up	TMPRSS4
11735633_a_at	1.5139756	up	RPS6KA5
11743911_a_at	-1.5697218	down	PLSCR1
11742811_at	1.8445395	up	RPS6KA3
11753900_x_at	-1.5936435	down	MT2A
11718217_at	1.6063756	up	RAB22A
11744131_a_at	1.5374482	up	SECISBP2L
11720625_a_at	-1.5944444	down	MAT2B
11733450_a_at	1.7828236	up	SLFN11
11738387_s_at	-1.6611612	down	IL28B
11718766_at	1.7928658	up	PRSS23
11761701_at	-1.5917621	down	AP4B1

11738387_s_at	-1.6611612	down	IL28A
11753549_a_at	-1.5002522	down	CMTM3
11754780_s_at	-1.5441613	down	ZNF767
11732426_a_at	2.0448902	up	GNA14
11721136_a_at	-2.0686736	down	CMC2
11734359_a_at	-1.7831321	down	RNASEL
11717792_a_at	-1.6400951	down	FAM219A
11750028_a_at	-1.6317904	down	ATP6AP2
11760122_at	-1.502225	down	RBM4
11749969_a_at	1.541634	up	TSPAN5
11724727_a_at	1.5159038	up	EIF5
11734203_at	-1.6215488	down	HBS1L
11731284_a_at	1.8523912	up	NR2E3
11732467_x_at	-1.6214824	down	CXCL11
11720298_at	-1.6095484	down	CXCL10
11755758_s_at	-1.6012666	down	NLRC5
11718859_a_at	1.545732	up	NUDCD3
11728180_s_at	-1.5033238	down	CHIC1
11758312_x_at	1.5214931	up	LOC100510707
11755485_a_at	1.667497	up	OPLAH
11734131_a_at	-1.6729615	down	SLC2A4
11763852_a_at	-1.7301892	down	ELOVL4
11734099_at	1.5606201	up	ZNF578
11725746_a_at	-1.55321	down	PITPNC1
11729564_s_at	-1.6470174	down	DND1
11721774_a_at	-1.8320252	down	ASPH
11747002_a_at	-1.6806082	down	CPA1
11717372_s_at	1.6968044	up	DNAJC3
11762449_x_at	-1.5235559	down	FNDC3B
11718166_a_at	1.5013912	up	RBL2
11735904_at	-2.009029	down	IL29
11716230_s_at	-1.9240552	down	TMEM167B
11737580_at	1.9197469	up	HLA-L
11716203_a_at	2.067123	up	MGP
11722000_a_at	1.5056927	up	HNRNPU
11760144_x_at	-1.5555491	down	HLA-F
11726673_s_at	1.5561081	up	ASCL1

11717885_a_at	-1.5584075	down	CCDC3
11715776_a_at	1.5629668	up	HSPB8
11761186_at	1.6662817	up	DDX31
11718722_at	2.0763202	up	PSCA
11738896_a_at	-1.504897	down	CD200R1L
11748379_a_at	1.5377399	up	SPATA13
11762420_at	-1.8730406	down	FBXO11
11723155_at	-1.5217113	down	CAMTA1
11759285_at	-1.6798565	down	TRAF2
11758627_s_at	-1.7611448	down	ASS1
11715670_a_at	-1.526163	down	IFITM1
11717218_a_at	1.6713617	up	STK10
11760678_at	1.8571134	up	PPIL2
11727514_at	1.5060053	up	TTC9
11732275_at	-2.4636617	down	CCL5
11743708_at	1.5032547	up	SYCP2
11758362_s_at	-1.6250266	down	EXTL2
11715436_at	2.4854238	up	TIMP3
11756072_s_at	-1.6168088	down	SAA2-SAA4
11731827_at	1.6081882	up	ZNF425
11760515_x_at	1.5441613	up	LIAS
11751629_a_at	-1.5365723	down	ASF1B
11723187_at	-1.7260405	down	FGD6
11738608_a_at	1.5425503	up	SYT10
11715846_at	-2.078534	down	EFEMP1
11758358_x_at	-1.7958246	down	LOC100653257
11759159_at	-1.55313	down	ABCB5
11733149_a_at	-1.9134078	down	DDX58
11743730_at	-1.5966345	down	TNFSF10
11725429_at	-2.4019895	down	LAMP3
11732875_s_at	1.6415458	up	GAGE13
11719394_a_at	1.6582521	up	FBXO32
11759287_at	1.8336581	up	DNAJB4
11738734_at	-1.55843	down	OR51A7
11763704_a_at	1.6418675	up	SAT1
11745918_a_at	1.5667238	up	USPL1
11751089_a_at	-1.5804669	down	VAR52

11742350_at	-1.5053624	down	OR52H1
11732414_a_at	-1.5794992	down	LRRRC8B
11726996_at	1.5729647	up	PINK1
11723234_at	-1.6982654	down	IFI44L
11732211_a_at	1.7599432	up	ZKSCAN1
11718933_s_at	2.1247606	up	SDCBP2
11735044_x_at	-2.1570575	down	TRIM5
11726286_a_at	-1.5056529	down	WARS
11718492_at	1.8807254	up	SLC1A2
11715287_at	-2.008598	down	C15orf40
11716939_a_at	4.6153255	up	HMOX1
11744236_a_at	-2.2392704	down	DDX60
11754043_a_at	1.5033376	up	RHOA
11757262_at	2.001951	up	SCARNA20
11732670_a_at	1.510727	up	CCDC107
11719171_a_at	1.6791202	up	AKR1C1
11732875_s_at	1.6415458	up	GAGE2A
11741642_s_at	1.7182286	up	ZFY
11741642_s_at	1.7182286	up	ZFX
11732875_s_at	1.6415458	up	GAGE2D
11732875_s_at	1.6415458	up	GAGE2E
11746779_a_at	-1.5228671	down	NCOA7
11732875_s_at	1.6415458	up	GAGE2B
11732875_s_at	1.6415458	up	GAGE2C
11724983_at	1.7069736	up	PCDH7
11741548_a_at	-1.5554962	down	MBNL1
11757747_s_at	-1.5072343	down	LPIN1
11737916_a_at	1.5561081	up	NEK11
11724776_at	1.5484667	up	PGM2L1
11723302_a_at	-1.515005	down	CHGA
11720709_x_at	1.5711502	up	KIF1B
11727871_at	-1.6536858	down	PPM1K
11753961_a_at	1.5845875	up	IGF2R
11757261_at	2.679615	up	SCARNA14
11736407_x_at	-1.6012063	down	XYLB
11718552_at	-1.6940216	down	OTUD4
11762431_at	-1.9333485	down	RSPH10B2

11725536_at	-1.5895256	down	ANKRD34A
11758026_s_at	-1.5436239	down	SLC35A5
11763493_at	1.5139756	up	KITLG
11722147_at	-1.613025	down	PAIP2B
11763134_at	-1.5457437	down	ZBTB8OS
11758358_x_at	-1.7958246	down	SHISA9
11751345_at	-1.5377406	down	LOC100288601
11739985_a_at	1.5939617	up	C1QTNF3
11731742_a_at	-1.5788311	down	TRDMT1
11737787_at	-1.6279392	down	SHISA5
11747630_a_at	-2.582074	down	XAF1
11730470_at	1.5768708	up	CALML5
11752395_a_at	1.5578084	up	NFATC1
11743763_at	-2.0596123	down	GTF3C3
11719021_at	-1.5147023	down	WDFY1
11728825_at	-1.5434579	down	TRNP1
11724134_a_at	1.5354971	up	SLC12A2
11763653_at	-1.6295229	down	TMC5
11763528_s_at	1.6420163	up	SLC12A4
11723819_at	1.5252402	up	PM20D2
11724688_a_at	-1.5427895	down	SAMD11
11744955_a_at	1.6282454	up	ANXA1
11739149_a_at	-1.870242	down	SAMHD1
11754485_x_at	1.5430986	up	SERHL
11722143_at	-1.7292973	down	TRANK1
11759424_at	-1.5158672	down	ANXA5
11741097_a_at	1.5271657	up	WBP1L
11726756_a_at	-1.6165959	down	CDC25A
11726013_a_at	-1.6338665	down	AJUBA
11731407_x_at	-2.0400043	down	IFIT3
11721873_at	-2.5552428	down	IFIT2
11725531_a_at	1.6854856	up	DSC2
11716663_a_at	2.2019424	up	GDF15
11751267_a_at	-1.6207311	down	ADAMDEC1
11723025_at	-1.5331683	down	FAM26F
11734646_a_at	1.5799824	up	TBL1Y
11717046_at	1.5150048	up	C11orf95

11755381_s_at	-1.5485424	down	PLGLA
11748907_a_at	-1.8995318	down	RARRES3
11726823_at	-1.6346554	down	ADORA3
11741375_a_at	-1.8004568	down	CADM1
11738061_a_at	-1.7727414	down	S100A7
11717971_s_at	-1.504552	down	FAM20B
11743632_a_at	1.6279392	up	PDLIM5
11759969_at	-1.567178	down	STAT5B
11729829_at	1.5072346	up	FAM110B
11721325_a_at	1.5155787	up	GCAT
11718933_s_at	2.1247606	up	FKBP1A-SDCBP2
11749609_s_at	-1.9774013	down	ZNF321P
11732418_at	1.6645896	up	FAM105A
11755739_a_at	-1.5163723	down	SLC35A1
11731756_at	-1.6712081	down	KLHDC7B
11731751_at	-2.0244453	down	RNF213
11756585_a_at	2.0022223	up	AQP3
11724435_a_at	1.6116029	up	TPK1
11715475_a_at	1.5115865	up	DDX17
11756065_x_at	1.622265	up	APOD
11748649_a_at	1.5163032	up	VPS13C
11753291_a_at	1.6002423	up	CD44
11727380_s_at	1.6368111	up	H2AFV
11745673_a_at	1.5382268	up	CEP290
11757018_a_at	-1.5765573	down	COL12A1
11729696_at	-1.5136784	down	C2orf69
11725844_at	-1.5895256	down	SREK1IP1
11720532_s_at	-1.5150048	down	C9orf72
11728908_at	-1.6425488	down	B3GALTL
11758358_x_at	-1.7958246	down	HERC2P4
11761176_at	1.5794997	up	POLL
11757977_s_at	1.7342886	up	SLC12A7
11755978_a_at	-1.5901604	down	GPR139
11747098_a_at	1.5120603	up	ATRNL1
11733425_at	-1.7840658	down	PMCH
11735340_a_at	1.5659783	up	TANC1
11760254_at	-2.2728531	down	IFI44

11759983_at	1.5484656	up	VTI1A
11719122_at	-2.0382485	down	DPCD
11743071_a_at	1.7182286	up	LPAR6
11742082_a_at	-1.8126485	down	LCTL
11740114_a_at	1.508913	up	CGN
11754404_a_at	-1.6384263	down	PARP14
11717582_a_at	2.200323	up	RGCC
11724197_at	-1.8377799	down	STC1
11738070_at	-1.7303679	down	HAS3
11734118_a_at	-1.5854865	down	BTN3A3
11751482_s_at	-1.7070782	down	BTN3A2
11739156_at	1.5218955	up	TMX4
11723699_s_at	-1.5923125	down	OAS3
11728318_at	-1.5066552	down	FAM122A
11757869_s_at	1.7715752	up	AKAP13
11719588_a_at	-1.5504394	down	OAS1
11740588_at	1.8670217	up	BDKRB2
11736135_at	-2.2997234	down	OAS2
11735549_at	-1.5794995	down	ASB15
11719491_a_at	-1.5019073	down	IFI35
11761371_at	-1.5096486	down	LOC100288974
11721046_a_at	1.5366892	up	SERINC2
11756346_a_at	1.5048964	up	FAM102B
11724128_a_at	1.7243507	up	FAM65C
11740385_x_at	-1.6458241	down	METTL20
11738398_a_at	-1.527669	down	LHX6
11735110_at	1.7109532	up	FBXO3
11735270_a_at	1.7763509	up	GCNT1
11749916_a_at	-1.5609139	down	AGBL2
11736223_a_at	1.5400368	up	IKZF5
11716094_a_at	1.5653361	up	KLF6
11759428_a_at	1.847737	up	KLF7
11735790_x_at	1.5460038	up	PTPN18
11733725_a_at	-1.6012888	down	CFB
11741492_x_at	-1.5732049	down	FAM111B
11732152_a_at	-1.6416047	down	AGBL5
11755739_a_at	-1.5163723	down	C6orf165

11731152_s_at	-1.5414933	down	LOC100288963
11735069_a_at	-1.534331	down	MYOZ3
11722290_a_at	1.5766139	up	ZBTB43
11756689_a_at	1.5479928	up	HN1L
11761907_at	-2.000634	down	NR1I3
11726364_x_at	-2.1203535	down	OASL
11733666_a_at	-1.553516	down	C14orf118
11727294_s_at	-1.5458648	down	ALG10
11723524_at	1.5538436	up	AGR3
11721805_at	1.5577254	up	KLF2
11745862_x_at	1.5153663	up	TCF12
11726523_s_at	1.5105537	up	ZFH3
11759733_a_at	2.0730584	up	FAM91A1
11721346_a_at	-1.5005612	down	MPEG1
11730510_at	1.6121413	up	EID2B
11762431_at	-1.9333485	down	RSPH10B
11749941_a_at	-1.8180891	down	FCRL6
11763901_s_at	1.5865077	up	MIR1248
11749551_a_at	1.5516154	up	RNGTT
11736667_a_at	1.5672898	up	PTER
11743537_a_at	-1.6190135	down	DNAJC18
11756072_s_at	-1.6168088	down	SAA2
11716127_a_at	1.5010756	up	BAG1
11756072_s_at	-1.6168088	down	SAA1
11728325_at	1.6391373	up	TTC30A
11756649_a_at	-1.5377262	down	SEH1L
11741874_x_at	1.8343076	up	SEPP1
11746710_a_at	1.5184673	up	DOCK10
11755207_a_at	-1.784256	down	NT5E
11758972_s_at	-1.5573337	down	ZNF354C
11755374_a_at	-1.5926452	down	HERC5
11726837_a_at	-1.5039828	down	SCAI
11738879_s_at	-1.6002032	down	PSG1
11743665_at	1.5120603	up	SPEN
11719641_at	-1.6025431	down	CDS1
11760265_at	-1.5485424	down	PIH1D2
11736246_a_at	-1.5273044	down	AMIGO2

11743843_a_at	1.5447664	up	DNAJC28
11738879_s_at	-1.6002032	down	PSG8
11748437_a_at	-1.5053464	down	SUSD4
11760356_at	-1.7369939	down	PMPCB
11759903_s_at	1.5208244	up	SDCCAG8
11718159_at	-1.5545962	down	NMI
11731673_at	-1.8829347	down	LCORL
11721711_at	-1.5555322	down	SHROOM3
11740387_at	-1.8528094	down	SHROOM4
11725444_at	-1.8800582	down	CCR1
11749609_s_at	-1.9774013	down	ZNF816-ZNF321P
11724118_a_at	-1.6428545	down	SAMD9L
11739338_at	-1.7075251	down	FAM46C
11758358_x_at	-1.7958246	down	LOC100652752
11761155_x_at	-1.6107235	down	DNALI1
11745908_a_at	1.5618565	up	KIAA0494
11721376_at	-1.8665177	down	BCL2
11747597_x_at	-1.6450691	down	CLEC2D
11756353_a_at	-1.6281167	down	CLVS1
11755381_s_at	-1.5485424	down	PLGLB2
11755381_s_at	-1.5485424	down	PLGLB1
11728377_x_at	-1.51824	down	NMU
11749184_a_at	1.6015323	up	DTNA
11749962_a_at	1.6818551	up	BCAS1
11733904_at	-1.5418	down	RRP15
11748674_x_at	1.5404018	up	AFF4
11732881_s_at	-1.528376	down	TBX1
11761339_s_at	-1.5218955	down	FAM115C
11758527_s_at	1.5247785	up	ITPR2
11755147_s_at	-1.5297607	down	STAT2
11743960_a_at	-2.1591318	down	SLC16A3
11757833_a_at	1.5003197	up	RAB31
11757626_x_at	-1.5485426	down	SLC16A4
11721540_a_at	1.5033367	up	MAPK13
11728497_s_at	1.593109	up	SVIL
11723854_at	-1.9397229	down	SAMD9
11730015_s_at	-1.7862935	down	NEUROD2

11722953_a_at	1.5645008	up	BIK
11759039_at	-1.5336275	down	SVIP
11759031_at	1.503131	up	ABCC2
11760976_a_at	-1.6035932	down	APBB1
11739985_a_at	1.5939617	up	C1QTNF3-AMACR
11760122_at	-1.502225	down	RBM14-RBM4
11744481_s_at	1.6383266	up	OPN3
11725890_s_at	1.591558	up	ABCC6
11750730_x_at	-1.6060029	down	SNCAIP
11763901_s_at	1.5865077	up	SNORD2
11732956_a_at	2.611227	up	TRGC2
11751345_at	-1.5377406	down	LOC653720
11730602_at	-1.5343305	down	APOBEC3F
11750916_a_at	1.5269173	up	FAM73A
11740498_at	-1.6798565	down	OCSTAMP
11731654_at	-1.7841289	down	ARL15
11761362_at	-1.7308421	down	RC3H2
11755962_a_at	-1.5890702	down	SLC25A28
11747171_a_at	1.5150193	up	MIR4800
11716167_a_at	-1.6644443	down	MX1
11726479_a_at	-3.7341619	down	MX2
11733446_at	-1.5313041	down	MMS22L
11751612_a_at	1.6898264	up	SOCS2
11717561_s_at	-1.5314788	down	DTX3L
11737146_a_at	-1.5072343	down	SOCS1
11736414_a_at	-1.5484738	down	MF12
11762200_a_at	1.5667523	up	QDPR
11746502_s_at	1.5352923	up	ZNF814
11749609_s_at	-1.9774013	down	ZNF816
11747419_a_at	-1.5856112	down	MOGS
11722462_a_at	-1.5609142	down	TNKS2
11732875_s_at	1.6415458	up	GAGE1
11716753_x_at	-1.6816461	down	GNS
11724444_a_at	-2.3173835	down	ASB9
11746470_a_at	1.5302902	up	MAP4K4
11723613_s_at	2.36594	up	SERHL2
11730556_s_at	-1.6752697	down	TRIM34

11724145_a_at	1.5210174	up	SLC37A1
11724594_at	1.9206458	up	HRASLS
11750561_a_at	1.968556	up	LYST
11733703_x_at	-1.5005615	down	SKIDA1
11754943_s_at	-1.5890423	down	SLC25A35
11722618_a_at	1.52914	up	RIPK4
11718140_a_at	1.6861918	up	EMP3
11741911_a_at	-1.937068	down	GBP3
11726329_x_at	-2.4962826	down	GBP1
11758312_x_at	1.5214931	up	TBC1D3C
11761451_a_at	-1.608481	down	FRAS1
11734764_at	-1.5578084	down	FGFR1
11758312_x_at	1.5214931	up	TBC1D3F
11758312_x_at	1.5214931	up	TBC1D3G
11754249_at	-1.5159029	down	WHAMMP3
11754249_at	-1.5159029	down	WHAMMP2
11758312_x_at	1.5214931	up	TBC1D3H
11759188_at	-2.3330567	down	ADCYAP1R1
11734725_a_at	-1.56782	down	PNPT1
11759756_x_at	1.6207311	up	ERVK-4
11725056_a_at	2.0414658	up	NEDD9
11756590_a_at	2.0443957	up	KMO
11758312_x_at	1.5214931	up	TBC1D3B
11723105_at	-2.2279956	down	CMPK2
11715386_at	1.6655086	up	REG1A
11751458_a_at	1.5140359	up	TRIM68
11729998_a_at	1.6276928	up	B3GNT7
11716787_a_at	-1.5892566	down	B3GNT1
11747584_a_at	-1.5396694	down	C8orf34
11739285_a_at	-2.0736902	down	ARL6IP6
11755242_a_at	1.5048966	up	SKIL
11726784_a_at	-1.5868516	down	LRFN5
11723689_at	-1.7726172	down	CREBL2
11716993_a_at	1.514477	up	CSF1R
11727256_a_at	-1.5657091	down	ZNF625-ZNF20
11760321_at	1.7642728	up	ZMYM6
11731795_at	1.6346389	up	EPHX4

11731626_a_at	1.631574	up	C10orf118
11747961_a_at	-1.7935131	down	PSMB8
11717305_a_at	1.7043141	up	C10orf116
11726677_a_at	-2.6678288	down	PSMB9
11762546_at	-1.5846977	down	FOXP2
11728328_at	-1.565735	down	OMD
11716721_a_at	1.7369939	up	PHF1
11748205_a_at	-1.8124828	down	EMR1
11739861_s_at	-1.5032542	down	ITGA6
11731940_a_at	1.5079535	up	UCP3
11759440_at	-1.5425503	down	GLS
11725890_s_at	1.591558	up	ABCC6P2
11739751_s_at	1.5005612	up	SLC25A16
11763901_s_at	1.5865077	up	SNORA4
11757114_at	2.0257478	up	SNORA12
11730580_s_at	1.5185711	up	HECW2
11758721_s_at	-1.6265365	down	IGFBP7
11759882_a_at	-1.5252619	down	EPS15L1
11733962_a_at	-1.6054096	down	LGR5
11745626_x_at	1.5014939	up	PCDHGA2
11748735_s_at	-1.5312763	down	BZW1
11748524_x_at	-1.6083131	down	PIGK
11738675_at	-1.5667517	down	OR5AU1
11757638_s_at	-1.9193801	down	CD93
11720779_a_at	1.5131972	up	KLHL22
11730237_at	-1.511095	down	ABHD10
11736998_at	-1.9019992	down	NIPAL1
11729691_a_at	1.6697279	up	KLHL24
11757953_x_at	-1.518893	down	TTC39C
11749525_a_at	-1.919745	down	AKT2
11733240_at	1.5989013	up	IRAK2
11721317_at	1.6791202	up	PARM1
11745313_a_at	1.5694313	up	SYNRG
11759828_s_at	-1.6099007	down	SP100
11761404_at	-1.5001551	down	RING1
11732946_a_at	-1.5794997	down	CCDC48
11742996_a_at	-1.6263968	down	MCM3

11764248_s_at	-1.5280077	down	LDLRAD3
11762549_at	-1.6151707	down	MCTP1
11760960_at	-1.5393246	down	EML2
11732956_a_at	2.611227	up	TARP
11735833_a_at	1.8177478	up	KIAA1199
11753940_a_at	-1.5004318	down	NRL
11759860_at	-1.7960498	down	GRIK1-AS2
11724414_a_at	-1.6084114	down	ZNF711
11738061_a_at	-1.7727414	down	S100A7A
11753819_a_at	1.5794413	up	MDM2
11764058_at	-1.8592995	down	PRNP
11739295_a_at	-1.535001	down	ICOSLG
11746429_a_at	-1.5315456	down	MDM1
11737466_at	-1.5049156	down	RUSC1-AS1
11716641_x_at	-1.5012879	down	PSMB10
11731461_x_at	1.9586015	up	CPM
11728879_at	1.6194615	up	PPP3R1
11739217_a_at	-2.117133	down	RSAD2
11717810_a_at	1.5485419	up	CYTH3
11758100_s_at	-1.7312346	down	C1S
11737927_a_at	1.5458275	up	C6orf141
11727782_a_at	1.7292653	up	TPM4
11756818_a_at	-1.8226013	down	PATL2
11722756_at	-1.9317051	down	TMEM37
11761420_a_at	-1.55843	down	RGS11
11746276_s_at	1.5951908	up	RGS12
11723059_a_at	-2.1235538	down	TAP2
11716680_x_at	-1.6993266	down	SLC39A9
11734514_a_at	-1.7520947	down	TEPP
11758075_s_at	-1.5542151	down	SLC18B1
11717840_at	-1.5747207	down	ETNK1
11716823_s_at	1.555981	up	BDH2
11734252_at	-1.6214824	down	TMEM87A
11727528_a_at	1.5050527	up	PHF20L1
11758589_s_at	-1.6464356	down	ERCC4
11718049_s_at	-1.5654712	down	GLRX
11742560_at	-1.7251763	down	OR6N2

11724836_at	-1.6752509	down	NCEH1
11747059_a_at	1.6867963	up	ZBTB7C
11739989_a_at	1.6365407	up	CPPED1
11727918_s_at	1.8226811	up	MUC20
11749229_a_at	-1.5459281	down	SIRT5
11727277_a_at	-1.5049156	down	TMEM169
11715432_a_at	1.5377399	up	TMBIM1
11716746_a_at	-1.5021089	down	FAM60A
11744178_a_at	-1.5834577	down	C19orf66
11743710_a_at	1.5285811	up	RGS22
11754555_x_at	1.5189155	up	CEP68
11759327_at	1.6405532	up	ATP8A2
11746122_s_at	1.525102	up	ZC3H11A
11758358_x_at	-1.7958246	down	LOC100422737
11740622_a_at	-1.7473027	down	GPR115
11728653_at	2.3421953	up	IGFBP5

DEGs, differentially expressed genes.